Joint Beamforming Design and Resource Allocation for Terrestrial-Satellite Cooperation System

Yuandong Zhang, *Student Member, IEEE*, Liuguo Yin, *Member, IEEE*, Chunxiao Jiang, *Senior Member, IEEE*, and Yi Qian, *Fellow, IEEE*

***Abstract*— In this paper, we investigate a multicast beamforming terrestrial-satellite cooperation system to optimize the communication capacity and quality of service. Different from traditional link-based terrestrial network, we design the terrestrial and satellite beamforming vectors cooperatively based on the required contents of users in order to realize more reasonable resource allocation. Meanwhile, the backhaul links between content provision center and satellite and base stations are limited, and the users always need high quality of service, considering these, our object is maximizing the sum of user minimum ratio under the constraints of resource allocation, backhaul link and quality of service in reality. We first formulate the optimization problem and propose a joint optimization iterative algorithm to design the beamforming vectors of satellite and base stations cooperatively. Then, to obtain the global optimum solution, we propose a Bound-based algorithm and solve the optimization problem by shrinking the upper bound and lower bound of the optimization feasible region. To decrease the complexity, we then design a heuristic scheme to solve the problem. The simulation results show that, our proposed cooperative optimization algorithms have better performance than non-cooperative methods, and the heuristic scheme has little poor performance but has significant advantage in low complexity.**

***Index Terms*— Terrestrial-satellite cooperation system, multicast, resource allocation, beamforming design, quality of service.**

I. Introduction

In RECENT years, the requirements of multimedia information such as music, video, mobile TV, online live show etc. increase rapidly [1]. According to the research in [1], in 2014, the mobile data flow was about 2.5EB and it was predicted to reach 24.3EB in 2019. And it is estimated that, by 2019, the video service ratio will ascend to 72 percent of total mobile services, which was only 55 percent in 2014. It is obviously that the mobile information today faces with the explosion of increment, which challenges the network transmission ability seriously. But the communication conditions such as frequency bandwidth, transmitting power, high interference and even hardware performance could not afford the high requirement of the information [2]. So the contradiction between huge demands for mobile information and the limited transmission resources is gradually significant.

One possible way to reduce the conflict is using the multi-input multi-output (MIMO) technology [3]–[6], especially in the Fifth Generation (5G) that massive MIMO had been considered as one of the most promising technologies [7], [8]. And it became the standard of the Third Generation Partnership Project (3GPP) [9]. In MIMO system, each base station is equipped with multi-antennas and serves multi-user equipments [10], which seems suitable for the huge demands of information and quality of service, but this technique still faces the challenge of power limitations, complex interference, transmission link limitations and so on [11]–[13]. To solve these problems, researchers studied in many fields that considered the application scenario as realistic as possible.

Beamforming is one of the important techniques to improve the quality of transmission [14], and the researchers in [15] proposed several beamforming methods. They described various beamforming algorithms that could be used in multiple-input single-output (MISO) orthogonal frequency-division multiplexing (OFDM) system, and they took both frequency and time domain correlation of channel fading into consideration. It is meaningful but the assumptions of the scenario are idealized. Later in [16], the author proposed a robust beamforming design algorithm to solve the max-min signal-to-interference-plus-noise ratio (SINR) problem that considered the interference. This model is more realistic but all of them are under the transmission of unicast. They could not use the communication channel best because each beam only served one user. So the researchers in [17]–[20] studied the multicast beamforming technologies in different aspects. Paper [17] focused on the quality of service (QoS) problem and max-min-fair (MMF) problem that they proposed a joint multicast beamforming design to improve QoS of users. The authors in [18] investigated a multicast beamforming method for multicell networks and considered the interferences

Manuscript received April 19, 2019; revised August 21, 2019; accepted October 18, 2019. Date of publication October 29, 2019; date of current version February 14, 2020. This work was supported by the National Natural Science Foundation of China (91538203 and 61871257), the new strategic industries development projects of Shenzhen City (JCYJ20170307145820484), the Joint Research Foundation of the General Armaments Department and the Ministry of Education (6141A02033322), and the Beijing Innovation Center for Future Chips, Tsinghua University. The associate editor coordinating the review of this article and approving it for publication was D. Niyato. *(Corresponding author: Liuguo Yin.)*

Y. Zhang is with the School of Aerospace Engineering, Tsinghua University, Beijing 100084, China, and also with the Key Laboratory of EDA, Research Institute of Tsinghua University in Shenzhen, Shenzhen 518057, China (e-mail: yd-zhang15@mails.tsinghua.edu.cn).

L. Yin and C. Jiang are with the School of Information Science and Technology, Tsinghua University, Beijing 100084, China, with the Beijing National Research Center for Information Science and Technology, Beijing 100084, China, and also with the Key Laboratory of EDA, Research Institute of Tsinghua University in Shenzhen, Shenzhen 518057, China (e-mail: yinlg@tsinghua.edu.cn; jchx@tsinghua.edu.cn).

Y. Qian is with the Department of Electrical and Computer Engineering, University of Nebraska-Lincoln, Omaha, NE 68182 USA (e-mail: yqian2@unl.edu).

Color versions of one or more of the figures in this article are available online at http://ieeexplore.ieee.org.

Digital Object Identifier 10.1109/TCOMM.2019.2950022

between groups. In [19], a multiuser beamforming and partitioning problem was proposed where the authors considered the SINR constraints in sum capacity maximization problem. And in [20], the authors proposed a multi-objective unicast and multicast beamforming optimization method under the constraints of backhaul link capacity. All of these works developed the multicast beamforming technologies in multi-user service that improved the information capacity and QoS notably. But they were all limited in the terrestrial network that the weaknesses of base-station-based transmission still influenced the performance of communication such as the limitation of coverage and so on.

Considering the wide coverage of the satellite, using the satellite networks could provide better service for ground users [21], [22]. In [23] a non-orthogonal multiple access (NOMA) based multimedia multicast beamforming Terrestrial-Satellite Network model was built. The users were divided into base station users and satellite users, meanwhile the satellite and the base stations were equipped with multi-antennas and could serve group users based on their required contents. It was pioneering but the cooperation of the satellite and base stations was not enough because the satellite only served the users far from the base stations. Later in [24], the authors proposed a joint beamforming design algorithm to maximize the minimum SINR users. In this literature, the satellite and base stations worked cooperatively that served all the users in the coverage, but the constraints of it were simple that the authors only keep the power of satellite and base stations under constraint. In the actual scenario, not only the power but also other factors such as backhaul link should be considered.

Motivated by the advantages of the satellite networks, in this paper, aiming at satisfying the high requirements of information capacity and users' QoS, we propose a joint beamforming design and resource allocation method in terrestrial-satellite cooperation system. We consider that, the satellite and the base stations could serve the ground users under coverage cooperatively based on the requirements of them. And to reduce the resource consuming, we reuse the frequency bandwidth and adopt multicast technology both in satellite and base stations transmission. Different from the aforementioned proposals, we focus on the demands of communication quantity and quality in actual scenario. Beside the user channel conditions, the peak transmission power of each base station and satellite, the backhaul link between the terrestrial-satellite system and the content provision center all influence the communication transmission quantity and quality, so we also optimize the target problem under the constraints of QoS and backhaul link capacity. Meanwhile, during the solution, we further consider the physical property of beams in order to obtain better system performance.

The main contributions of this paper are summarized as follows:

- We propose a model of joint beamforming design and resource allocation in terrestrial-satellite cooperation system, in which the satellite and base stations provide service cooperatively. We consider the maximization of sum user minimum ratio in order to satisfy the high demand of information capacity. To make the scenario more realistic, we also consider the constraints of backhaul link and the quality of service to achieve the requirement of the limited resources.
- We propose a joint iterative beamforming design and resource allocation algorithm to solve the optimization problem, in which we design the beamforming vectors of satellite and base stations cooperatively according to the requirement and constraints, and allocate the resources according to the users' condition. The proposed method is based on the Successive Convex Approximation (SCA) approach and iteration method.
- We propose a bound-based algorithm to obtain the bound of the optimization problem and solve the global optimization result. During the solution, we further consider the physical property of beams to obtain a better performance. The solution of this algorithm could be treated as the benchmark for evaluating the performance of sub-optimization method for the same problem that have the same target. Later we design a heuristic low-complexity algorithm by transforming the constraints into difference form to decrease algorithm complexity.

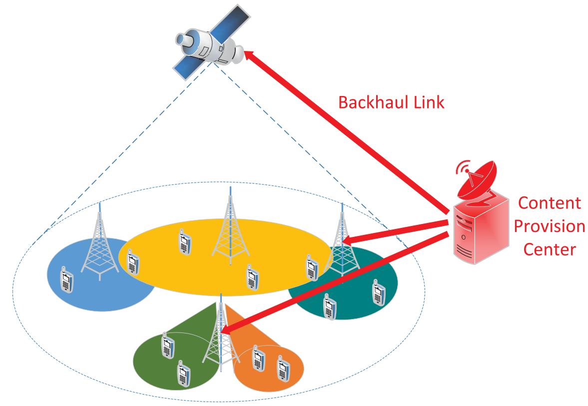

Fig. 1. The terrestrial-satellite cooperation system.

The rest of the paper is organized as follows. In Section II, the system model and the problem formulation are presented. In Section III, the proposed joint iterative algorithm based on SCA is adopted to solve the joint optimization problem. In Section IV, the bound-based algorithm and a low-complexity algorithm are proposed to obtain the benchmark of the optimization problem. In Section V, we simulate the algorithms and give the results of the proposed algorithms. Finally, we conclude this paper in Section VI.

II. System Model and Problem Formulation

A. System Model

Fig.1 shows a Terrestrial-Satellite Cooperation System model of multicast multigroup communication architecture. In this system one satellite and I_B base stations serve ground users cooperatively. All users are under coverage of the satellite, and could be served more than one base stations according to their requirement. Then we divide these users into J_G groups totally based on their desired contents. Under this circumstance, the satellite not only provides the desired contents to the users but also promotes the quality of service of the bottleneck users. In this paper, we assume the satellite to be a low earth orbit (LEO) satellite. Further more, we assume the user number of each group is K_U and the total user number is K_{total} that $I_B \times J_G \times K_U = K_{total}$. Each base station has A_B antennas, the satellite has A_S antennas, the maximum user number in one group is M_U, the satellite and the base stations use the same spectrum during entire transmission. So the interferences appear among different groups of one base station, different groups of different base station and the satellite. Besides, there exist backhaul links between the content provision center and the satellite and base stations.

It is denoted that $\omega_{i,j}$ is the beamforming vector for base station i group j, and $\|\omega_{i,j}\|^2 = P_{B,i,j}$ which is the transmission power of group j in base station i. $x_{B,i,j}$ is the multicast signal serving group j, and $E[|x_{B,i,j}|^2] = 1$. Therefore, the transmission signal of base station i can be written as

$$s_{B,i} = \sum_{j=1}^{J_B} \omega_{i,j} x_{B,i,j} \tag{1}$$

We notice that, in the multicast transmission condition, the users that request same content may not distribute in same area. It seems that users in different areas with different channel condition are served by different beams is a better solution. From [24], for different beams that serve users with same contents, the beam vectors could be combined. So at the end, only one beamforming vector serves the users who require the same content is enough. So the beamforming vector in equation (1) is such a formulation.

For the satellite, the transmission signal can be written similarly as

$$s_S = \sum_{j=1}^{J_S} \nu_j x_{S,j} \tag{2}$$

where ν_j is the beamforming vector for group j, and $\|\nu_j\|^2 = P_{S,j}$ which is the transmission power of group j. $x_{S,j}$ is multicast signal serving group j, and $E[|x_{S,j}|^2] = 1$.

Then the received signal of base station user K in group J of base station I is

$$y_{I,J,K} = \sum_{i=1}^{I_B} h_{i,I,J,K}^H \omega_{i,J} x_J + g_{I,J,K}^H \nu_J x_J + \sum_{i=1}^{I_B} h_{i,I,J,K}^H \times \sum_{\substack{j=1 \\ j \neq J}}^{J_G} \omega_{i,j} x_j + g_{I,J,K}^H \sum_{\substack{j=1 \\ j \neq J}}^{J_G} \nu_j x_j + n_{I,J,K} \tag{3}$$

where $h_{i,I,J,K}$ is the channel from base station i to the user K in base station I group J, $g_{I,J,K}$ is the channel from satellite to the user K in base station I group J. $n_{I,J,K}$ is the AWGN noise. x_j is the required multicast signal of group j that $E[|x_j|^2] = 1$. In the equation (3), the first two parts are the required signal from the base station I, other base stations and the satellite. The third and fourth parts are the interferences from the base stations and the satellite.

So the SINR of user K of group J in base station I is

$$\gamma_{I,J,K} = \frac{|\mathcal{S}|^2}{\sum_{\substack{j=1 \\ j \neq J}}^{J_G} |\mathcal{I}|^2 + \sigma_N^2} \tag{4}$$

where we denote

$$\mathcal{S} = \sum_{i=1}^{I_B} h_{i,I,J,K}^H \omega_{i,J} + g_{I,J,K}^H \nu_J$$
$$\mathcal{I} = \sum_{i=1}^{I_B} h_{i,I,J,K}^H \omega_{i,j} + g_{I,J,K}^H \nu_j \tag{5}$$

Based on Shannon's Theorem, the capacity can be calculated by

$$R_{I,J,K} = \log_2(1 + \gamma_{I,J,K}) \tag{6}$$

where $R_{I,J,K}$ is the capacity of user K in group J from base station I including the signal from base stations and the satellite.

In the system model, there exist backhaul links that connect the content provision center and the satellite and base stations, so this link should be described in correct form. We assume the finite backhaul capacity as C_I in which $I \in [0, I_B]$ and $I = 0$ represents the satellite. This means that if the network resources have been occupied completely, the peak backhaul capacity is no more than C_I. Because the backhaul link capacity is limited that each base station or the satellite may not have the ability to serve all the user groups under the coverage, there needs a factor to represent the groups that have the ability to be served. We denote a binary variable s_J as the backhaul link enable factor. If $s_J = 1$, the group J could be served by the base stations or the satellite, and $s_J = 0$ otherwise. Under these assumptions, the backhaul constraint could be formulated as

$$\sum_{J=1}^{J_G} s_J R_{B,I,J,K} \leq C_I, \quad I \in [0, I_B] \tag{7}$$

where $R_{B,I,J,K}$ is the capacity of each base station or the satellite. The equation (4) shows the SINR of the user that served by the base stations and the satellite cooperatively. According to the actual scenario that each base station and the satellite all have their own backhaul link that connect to the content provision center, so we should to formulate them separately. Referring to the equation (4), we could give the backhaul capacity of each base station as

$$R_{B,I,J,K} = \log_2\left(1 + \frac{|\sum_{i=1}^{I_B} h_{I,i,J,K}^H \omega_{i,J}|^2}{\sum_{\substack{j=1 \\ j \neq J}}^{J_G} |\sum_{i=1}^{I_B} h_{I,i,J,K}^H \omega_{i,j} + g_{I,J,K}^H \nu_j|^2 + \sigma_N^2}\right) \tag{8}$$

where $h_{I,i,J,K}$ is the channel from base station I to the user k in base station i group J.

Same as the base station, the backhaul capacity of satellite is

$$R_{B,I,J,K} = \log_2\left(1+\frac{|g^H_{I,J,K}\nu_J|^2}{\sum_{\substack{j=1\\ j\neq J}}^{J_G}|\sum_{i=1}^{I_B} h^H_{I,i,J,K}\omega_{i,j} + g^H_{I,J,K}\nu_j|^2+\sigma_N^2}\right) \quad (9)$$

B. Problem Formulation

According to the requirements of the terrestrial-satellite cooperation system, our object is to maximize the sum rate of the users in each group of the cooperative system through the joint resource allocation and beamforming vectors design of base stations and satellite.

Considering that, our system model is based on multicast technology, so the capacity of each group is decided by the users who are under the worst channel condition or the worst SINR. And we know that, the power of the base stations and the satellite couldn't be unconstraint. In fact, the total power constraint of each base station and even the satellite is very strict. So the optimization problem could be formulated as (OP) below:

$$(OP) \quad \max_{\{\omega_j\}_{j=1}^{J_G},\{\nu_j\}_{j=1}^{J_G}} \sum_{j=1}^{J_G}\log_2(1+\min_{I,J,K}\gamma_{I,J,K})$$
$$s.t.\ C1:\ P_{B,I}=\sum_{j=1}^{J_G}||\omega_{I,j}||^2\le P_{B,i,I,max}\quad I\in[1,I_B]$$
$$C2:\ P_S=\sum_{j=1}^{J_G}||\nu_j||^2\le P_{S,max}$$
$$C3:\ \sum_{J=1}^{J_G}s_J R_{B,I,J,K}\le C_I\quad I\in[0,I_B]$$
$$C4:\ \min_{I,J,K}\gamma_{I,J,K}\ge\gamma_{0,J}\quad I\in[1,I_B]J\in[1,J_G]K\in[1,K_U]$$

which $C1$ and $C2$ are the constraints of the base stations and satellite. $C3$ is the constraint of the backhaul link capacity that illustrated above, and $I = 0$ means the backhaul link capacity of the satellite. $C4$ is the SINR constraints that keep the fairness of the users under different channel conditions.

Obviously, the optimization problem (OP) couldn't be solved directly because the optimization target and the constraints are non-convex, so we should transmit the optimization problem into convex form and then solve it.

III. The Joint Resource Allocation and Beamforming Design Algorithm

In this section, we propose a joint iterative algorithm to solve the resource allocation and beamforming design optimization problem that formulated as (OP). Considering the problem is non-convex, we first relax the problem into a convex form with successive convex approximation (SCA) and then solve it by the proposed iteration algorithm.

A. Convex-Relaxation of the (OP)

The original optimization problem (OP) is non-convex-optimization, the complexity and computation are difficult to use the violent-search. First we should relax the optimization problem (OP) in suitable method. The optimization target is a mix of maximize-minimum problem that we could not solve it directly. Observing the optimization target and the SINR fairness constraint $C4$, we could rewrite the optimization target as

$$\max_{\{\omega_j\}_{j=1}^{J_G},\{\nu_j\}_{j=1}^{J_G},\gamma_{0,J}} \sum_{j=1}^{J_G}\log_2(1+\gamma_{0,J})$$

Meanwhile, considering that our optimization problem is under multigroup scenario, similar to the existing works on multi-group problem [17], [25], we define $\Gamma_{I,J,K}$ as a target SINR factor of all individual users. In other words, the value of $\Gamma_{I,J,K}$ represents the grade of service of different groups.

Thus, the problem (OP) could be transmitted as

$$(OP1) \quad \max_{\{\omega_j\}_{j=1}^{J_G},\{\nu_j\}_{j=1}^{J_G},\gamma_{0,J}} \sum_{j=1}^{J_G}\log(1+\gamma_{0,J})$$
$$s.t.\ C1:\ P_{B,I}=\sum_{j=1}^{J_G}||\omega_{I,j}||^2\le P_{B,i,I,max}\quad I\in[1,I_B]$$
$$C2:\ P_S=\sum_{j=1}^{J_G}||\nu_j||^2\le P_{S,max}$$
$$C3:\ \sum_{J=1}^{J_G}s_J R_{B,I,J,K}\le C_I\quad I\in[0,I_B]$$
$$C4:\ \frac{\gamma_{I,J,K}}{\Gamma_{I,J,K}}\ge\gamma_{0,J}\quad I\in[1,I_B]J\in[1,J_G]K\in[1,K_U]$$

where the new constraint $C4$ means that the SINR of all the users under different grade of service in base station I group J are larger than the minimum SINR $\gamma_{0,J}$.

To simplify the expression, here we define two auxiliary variables $\Omega_{joint,J}$ and $h_{joint,I,J,K}$ as

$$\Omega_{joint,J} = [\nu_J^H,\omega^H_{1,J},\omega^H_{2,J},\ldots,\omega^H_{I_B,J}]^H$$
$$h_{joint,I,J,K} = [g^H_{I,J,K},h^H_{1,I,J,K},h^H_{2,I,J,K},\ldots,h^H_{I_B,I,J,K}]^H$$
$$||\Omega_{joint,J}||^2 = tr(\Omega^H_{joint,J}\Omega_{joint,J})$$
$$|h^H_{joint,I,J,K}\Omega_{joint,J}|^2 = tr(h^H_{joint,I,J,K}h_{joint,I,J,K}\Omega^H_{joint,J}\Omega_{joint,J})$$

So we could rewrite the constraint $C1$ and $C2$ of $(OP1)$ as

$$P_{B,I}=\sum_{j=1}^{J_G}tr(A_{B,I}\Omega^H_{joint,j}\Omega_{joint,j})\le P_{B,i,I,max}\ I\in[1,I_B]$$
$$P_S=\sum_{j=1}^{J_G}tr(A_S\Omega^H_{joint,J}\Omega_{joint,J})\le P_{S,max}$$

where we denote $A_{B,I} = \mathcal{D}iag\{\ldots, Z_1, \ldots, Z_2\}$, $A_S = \mathcal{D}iag\{\ldots, Z_3, \ldots, Z_4\}$, in which $Z_1 = I_{A_B \times A_B}$, $Z_2 = 0_{A_S \times A_S}$, $Z_3 = 0_{A_B \times A_B}$ and $Z_4 = I_{A_S \times A_S}$.

For the constraint $C3$, there exits a binary variable $s_J = \{0, 1\}$ that makes the constraint non-convex. From the previous definition, we know that if the group J is under service the factor $s_J = 1$, otherwise $s_J = 0$. Considering the transmission program, the cooperative system serve the users all by multicast. That indicates no matter $s_J = 0$ or 1, if the beamforming vector of group J equals to 0 ($\omega_{I,j} = 0$ or $\nu_j = 0$), the group J is not under service. So referring to the existing works [26], [27], we could rewrite the factor s_J in $C3$ as

$$\left\|||A_J\Omega_{joint,J}||_2^2\right\|_0 = \left\|tr(A_J\Omega_{joint,J}^H\Omega_{joint,J})\right\|_0$$

in which $A_J = \{0_1, \ldots, 0_{J-1}, 1_J, 0_{J+1}, \ldots, 0_{J_G}\}$. So the constraint $C3$ could be rewrite as

$$\sum_{J=1}^{J_G}\left\|tr(A_J\Omega_{joint,J}^H\Omega_{joint,J})\right\|_0 R_{B,I,J,K} \leq C_I I \in [0, I_B]$$

Although we use the l_0-norm to represent the binary variable s_J, it is still non-convex. So we should approximate it into a convex form. We define

$$u_J^{(t+1)} = \frac{1}{tr(A_J\Omega_{joint,J}^{(t)H}\Omega_{joint,J}^{(t)}) + \tau}$$

in which τ is a very small predetermined parameter, and t represents the iteration time when calculating the factor u_J by means of iteration algorithm. So the l_0-norm $\left\|tr(A_J\Omega_{joint,J}^H\Omega_{joint,J})\right\|_0$ could be rewrite as $u_J^{(t+1)}tr(A_J\Omega_{joint,J}^H\Omega_{joint,J})$.

Then we focus on the other factor $R_{B,I,J,K}$ in constraint $C3$. Although $R_{B,I,J,K}$ is decided by the groups under the service of base station I in the backhaul constraint, it is determined by the minimum users in each group as well. Because of the optimization of the problem is joint beamforming design, we only consider the quality of service of users under the base stations and satellite cooperative service. So the factor $R_{B,I,J,K}$ is also influenced by the optimization factor $\gamma_{0,J}$ which including the optimum ω and ν. Here we represent the $R_{B,I,J,K}$ as $\log(1+\gamma_{0,J}^*)$ that for base stations $\gamma_{0,J}^* = \gamma_{0,J}(\omega)$ and $\gamma_{0,J}^* = \gamma_{0,J}(\nu)$. So we could further rewrite the constraint $C3$ as

$$\sum_{J=1}^{J_G} u_J^{(t+1)}tr(A_J\Omega_{joint,J}^H\Omega_{joint,J})\log(1+\gamma_{0,J^*}) \leq C_I$$

But the logarithm $\log(1+\gamma_{0,J^*})$ is still non-convex. We adopt the Taylor expansion to approximate it into its first order below:

$$\begin{aligned}&\sum_{J=1}^{J_G} u_J^{(t+1)}\log(1+\gamma_{0,J^{*(t)}})tr(A_J\Omega_{joint,J}^H\Omega_{joint,J})\\&\quad+\sum_{J=1}^{J_G} u_J^{(t+1)}tr(A_J\Omega_{joint,J}^{(t)H}\Omega_{joint,J}^{(t)})\frac{\gamma_{0,J^*}-\gamma_{0,J^{*(t)}}}{\ln 2(1+\gamma_{0,J^{*(t)}})}\\&\quad-C_I \leq 0\end{aligned} \tag{10}$$

For the constraint $C4$ in $(OP1)$, its full form is

$$\frac{1}{\Gamma_{I,J,K}}\frac{|h_{joint,I,J,K}\Omega_{joint,J}|^2}{\sum_{\substack{j=1\\j\neq J}}^{J_G}|h_{joint,I,J,K}\Omega_{joint,J}|^2+\sigma_N^2} \geq \gamma_{0,J}$$

We introduce two auxiliary factors $\{\psi_{I,J}, \phi_{I,J}\}$ and rewrite it as:

$$\frac{1}{\Gamma_{I,J,K}}tr(h_{joint,I,J,K}^H\Omega_{joint,J}^H\Omega_{joint,J}h_{joint,I,J,K}) \geq \psi_{I,J},$$

$$\sum_{\substack{j=1\\j\neq J}}^{J_G}tr(h_{joint,I,J,K}^H\Omega_{joint,J}^H\Omega_{joint,J}h_{joint,I,J,K}) + \sigma_N^2 \leq \phi_{I,J},$$

$$\frac{\psi_{I,J}}{\phi_{I,J}} - \gamma_{0,J}^* \geq 0$$

According to [24], the term $\frac{\psi_{I,J}}{\phi_{I,J}}$ above is non-convex. Here we transmit it by using logarithm relaxation:

$$\ln(\gamma_{0,J}^*) + \ln(\phi_{I,J}) - \ln(\psi_{I,J}) \leq 0$$

Same as the approximation of logarithm, we use Taylor series expansion to transmit it into

$$\begin{aligned}&\ln(\gamma_{0,J}^{*(t)}) + \frac{1}{\gamma_{0,J}^{*(t)}}(\gamma_{0,J}^* - \gamma_{0,J}^{*(t)}) + \ln(\phi_{I,J}^{(t)})\\&\quad+\frac{1}{\phi_{I,J}^{(t)}}(\phi_{I,J}-\phi_{I,J}^{(t)}) - \ln(\psi_{I,J}) \leq 0\end{aligned} \tag{11}$$

in which $\gamma_{0,J}^{*(t)}, \phi_{I,J}^{(t)}$ are the optimum solutions from the t-times iteration.

Up to here, we have approximated all the constraints into convex form, so the optimization problem $(OP1)$ could be rewrite as

$$(OP2) \quad \max_{\{\omega_j\}_{j=1}^{J_G},\{\nu_j\}_{j=1}^{J_G},\gamma_{0,J},\psi,\phi} \sum_{j=1}^{J_G}\log(1+\gamma_{0,J})$$

$$\begin{aligned}s.t.\ C1:\ & P_{B,I} = \sum_{j=1}^{J_G}tr(A_{B,I}\Omega_{joint,j}^H\Omega_{joint,j})\\&\leq P_{B,i,I,max} I \in [1, I_B]\\C2:\ & P_S = \sum_{j=1}^{J_G}tr(A_S\Omega_{joint,J}^H\Omega_{joint,J})\\&\leq P_{S,max}\\C3:\ & \sum_{J=1}^{J_G}u_J^{(t+1)}\log(1+\gamma_{0,J^{*(t)}})\\&\times tr(A_J\Omega_{joint,J}^H\Omega_{joint,J})\\&+\sum_{J=1}^{J_G}u_J^{(t+1)}tr(A_J\Omega_{joint,J}^{(t)H}\Omega_{joint,J}^{(t)})\\&\times\frac{\gamma_{0,J^*}-\gamma_{0,J^{*(t)}}}{\ln 2(1+\gamma_{0,J^{*(t)}})} - C_I \leq 0\\C4:\ & \ln(\gamma_{0,J}^{*(t)}) + \frac{1}{\gamma_{0,J}^{*(t)}}(\gamma_{0,J}^* - \gamma_{0,J}^{*(t)})\\&+\ln(\phi_{I,J}^{(t)}) + \frac{1}{\phi_{I,J}^{(t)}}(\phi_{I,J}-\phi_{I,J}^{(t)})\\&-\ln(\psi_{I,J}) \leq 0\end{aligned}$$

Algorithm 1 Joint Optimization Iterative Algorithm

Initialize: C_I, σ, $h_{joint,I,J,K}$, $P_{B,i,I,max}$, $P_{S,max}$, $\Gamma_{I,J,K}$, set $t = 0$, and compute $\{\gamma_{0,J}^{(0)}, \phi_{I,J}^{(0)}\}$ according to (12), solve the initial problem of (OP2). Compute $u_J^{(1)}$ according to (10).
while Ω converge, $\forall I, J, K$ **do**
    Solve the SDP problem $(OP2)^{(t)}$ and calculate $\Omega_{joint,J}^{(t)}$, $\phi_{I,J}^{(t)}$ and $\gamma_{0,J}^{(t)}$.
    Update u_J^t according to (10)
    Rebuild the iteration optimization problem $(OP2)^{(t+1)}$ by $\Omega_{joint,J}^{(t)}$, $\phi_{I,J}^{(t)}$ and $\gamma_{0,J}^{(t)}$.
    t = t + 1
End While

B. Joint Optimization Iterative Algorithm

The optimization problem $(OP2)$ is approximated as a standard SDP problem according to [28], and could be solved by the CVX [29] tools. Before solving the problem $(OP2)$, we should initialize all the iteration factors, especially $\{\gamma_{0,J}^{(0)}, \phi_{I,J}^{(0)}\}$ and $u_J^{(0)} = \frac{1}{tr(A_J \Omega_{joint,J}^{(0)H} \Omega_{joint,J}^{(0)}) + \tau}$. We give the complete joint beamforming design and resource allocation iterative algorithm as **Algorithm 1**.

IV. Extend Bound-Based Algorithm

In the previous sections, we formulated a joint resource allocation and beamforming design problem to maximize the sum of user minimum rate with the requirement of massive information, and we proposed a joint iterative algorithm to solve the problem. The complexity of the algorithm is not very large and could converge to a point in several times that would be showed in Section V. But the performance might have room for improvement.

This is because when we solved the problem (OP) by using iterative method, we did not calculate the bound of the problem. That means we could not directly measure whether the performance of the algorithm reaches its limit. On the one hand, the optimization result of iterative method has possibility that gets stuck in unfavorable local solutions. On the other hand, two nested while-loop might obtain the sub-optimal solution instead of global solution. Thus, it is necessary to find a method that correctly describes the benchmark of the performance. So in this section, we try to find an algorithm to achieve this target.

To facilitate the following description, we rewrite the optimization problem below as $(EOP1)$.

$$
\begin{aligned}
(EOP1) \quad & \max_{\{\omega_j\}_{j=1}^{J_G}, \{\nu_j\}_{j=1}^{J_G}, \gamma_{0,J}} \sum_{j=1}^{J_G} \log(1+\gamma_{0,J}) \\
s.t.\ C1: \quad & P_{B,I} = \sum_{j=1}^{J_G} ||\omega_{I,j}||^2 \le P_{B,i,I,max} \\
& I \in [1, I_B] \\
C2: \quad & P_S = \sum_{j=1}^{J_G} ||\nu_j||^2 \le P_{S,max} \\
C3: \quad & \sum\nolimits_{J=1}^{J_G} s_J R_{B,I,J,K} \le C_I \\
& I \in [0, I_B] \\
C4: \quad & \frac{\gamma_{I,J,K}}{\Gamma_{I,J,K}} \ge \gamma_{0,J} \\
& I \in [1, I_B] J \in [1, J_G] K \in [1, K_U]
\end{aligned}
$$

Then we relax and solve it in the next two subsections.

A. Relaxation and Bound-Based Algorithm

First we focus on the constraint $C4$ that

$$
\frac{1}{\Gamma_{I,J,K}} \frac{|\sum_{i=1}^{I_B} h_{i,I,J,K}^H \omega_{i,J} + g_{I,J,K}^H \nu_J|^2}{\sum_{\substack{j=1 \\ j\neq J}}^{J_G} |\sum_{i=1}^{I_B} h_{i,I,J,K}^H \omega_{i,j} + g_{I,J,K}^H \nu_j|^2 + \sigma_N^2} \ge \gamma_{0,J} \tag{12}
$$

To simplify the expression, $C4$ could be rewritten as

$$
\frac{1}{\Gamma_{I,J,K}} \frac{|h_{joint,I,J,K} \Omega_{joint,J}|^2}{\sum_{\substack{j=1 \\ j\neq J}}^{J_G} |h_{joint,I,J,K} \Omega_{joint,J}|^2 + \sigma_N^2} \ge \gamma_{0,J} \tag{13}
$$

Then we define

$$
\mathcal{F}(\Omega_{joint,J}) = \Gamma_{I,J,K} \left(\sum_{\substack{j=1 \\ j\neq J}}^{J_G} |h_{joint,I,J,K} \Omega_{joint,J}|^2 + \sigma_N^2 \right)
$$

so $C4$ could be further rewritten as

$$
|h_{joint,I,J,K} \Omega_{joint,J}| \ge \sqrt{\gamma_{0,J}} \sqrt{\mathcal{F}(\Omega_{joint,J})} \tag{14}
$$

According to the previous research [20], [23], we know that, the argument of $|h_{joint,I,J,K} \Omega_{joint,J}|$ that we denote as $\theta_{I,J,K}$ have the range of $[\underline{\theta}_{I,J,K}, \bar{\theta}_{I,J,K}]$, $0 \le \underline{\theta}_{I,J,K} \le \bar{\theta}_{I,J,K} < 2\pi$. And we denote $\mathcal{W}_{I,J,K}^{[\underline{\theta}_{I,J,K}, \bar{\theta}_{I,J,K}]}(\gamma_{0,J})$ as the set of $\Omega_{joint,J}$ and $\gamma_{0,J}$ that have the inequality of $|h_{joint,I,J,K} \Omega_{joint,J}| \ge \sqrt{\gamma_{0,J}} \sqrt{\mathcal{F}(\Omega_{joint,J})}$. Suppose that $\bar{\theta}_{I,J,K} - \underline{\theta}_{I,J,K} \le \pi$, then we could get the convex envelope of $\mathcal{W}_{I,J,K}^{[\underline{\theta}_{I,J,K}, \bar{\theta}_{I,J,K}]}(\gamma_{0,J})$ as

$$
\begin{aligned}
& \mathcal{C}onv\left(\mathcal{W}_{I,J,K}^{[\underline{\theta}_{I,J,K}, \bar{\theta}_{I,J,K}]}(\gamma_{0,J}) \right) \\
& = \Big\{ \Omega_{joint,J} | \sin(\underline{\theta}_{I,J,K}) \mathcal{R}e\{h_{joint,I,J,K} \Omega_{joint,J}\} \\
& \quad - \cos(\underline{\theta}_{I,J,K}) \mathcal{I}m\{h_{joint,I,J,K} \Omega_{joint,J}\} \le 0, \\
& \quad \sin(\bar{\theta}_{I,J,K}) \mathcal{R}e\{h_{joint,I,J,K} \Omega_{joint,J}\} \\
& \quad - \cos(\bar{\theta}_{I,J,K}) \mathcal{I}m\{h_{joint,I,J,K} \Omega_{joint,J}\} \ge 0, \\
& \quad x_{I,J,K} \mathcal{R}e\{h_{joint,I,J,K} \Omega_{joint,J}\} \\
& \quad + y_{I,J,K} \mathcal{I}m\{h_{joint,I,J,K} \Omega_{joint,J}\} \\
& \ge (x_{I,J,K}^2 + y_{I,J,K}^2) \sqrt{\gamma_{0,J}} \sqrt{\mathcal{F}(\Omega_{joint,J})} \Big\}
\end{aligned} \tag{15}
$$

where $x_{I,J,K} = \frac{\cos(\underline{\theta}_{I,J,K}) + \cos(\bar{\theta}_{I,J,K})}{2}$ and $y_{I,J,K} = \frac{\sin(\underline{\theta}_{I,J,K}) + \sin(\bar{\theta}_{I,J,K})}{2}$. $\mathcal{C}onv()$ is the convex envelope factor, $\mathcal{R}e()$ and $\mathcal{I}m()$ means the real part and the imaginary part.

From the formulation above, it is easy to verify that, the smaller the difference value of $[\underline{\theta}_{I,J,K}, \bar{\theta}_{I,J,K}]$, the tighter the convex envelope of $\mathcal{W}_{I,J,K}^{[\underline{\theta}_{I,J,K}, \bar{\theta}_{I,J,K}]}(\gamma_{0,J})$.

Respectively, according to the previous analysis, the set of the convex envelope with the given $\underline{\gamma}_{0,J}$ could be written as

$$\Omega_{joint,J} \in \mathcal{C}onv\left(\mathcal{W}_{I,J,K}^{[\underline{\theta}_{I,J,K},\bar{\theta}_{I,J,K}]}(\underline{\gamma}_{0,J})\right) \tag{16}$$

and the convex envelope exists only when $\bar{\theta}_{I,J,K}-\underline{\theta}_{I,J,K} \leq \pi$.

The constraint $C3$ is the backhaul link capacity constraint for each base station and satellite. But there is a binary variable s_J in it, so it is non-convex and couldn't be solved easily. From [30], we denote a region that $G = \{(a,b)|a,b \in \mathbb{R}^n, \underline{a} \leq a \leq \bar{a}, \underline{b} \leq b \leq \bar{b}\}$. So the convex envelope of $f = a^H b$ in G have

$$\mathcal{C}onv_G(a^H b)=\sum_i\{\underline{b}_i a_i+\underline{a}_i b_i-\underline{a}_i\underline{b}_i, \bar{b}_i a_i+\bar{a}_i b_i-\bar{a}_i\bar{b}_i\} \tag{17}$$

Then we relax $s_J = \{0,1\}$ into a continuous form $s_J = [0,1]$, so the summation of each user equals to the product. According to the equation above, we could relax the $C3$ as

$$\begin{aligned}&\sum_{J=1}^{J_G}\{\underline{R}_{B,I,J,K}s_J + \underline{s}_J R_{B,I,J,K} - \underline{s}_J\underline{R}_{B,I,J,K},\\ &\quad \bar{R}_{B,I,J,K}s_J + \bar{s}_J R_{B,I,J,K} - \bar{s}_J\bar{R}_{B,I,J,K}\} \leq C_I\\ &\quad I \in [0, I_B]\end{aligned} \tag{18}$$

Here we recall the constraints $C1$ and $C2$, to relax the other constraints of (EOP), we redefine the beamforming vectors $\omega_{I,J}$ and ν_J as $\Omega_{joint,J}$, and use it in the relaxation form of convex envelope. So we need to rewrite $C1$ and $C2$ into a suitable form. We denote $A_{B,I} = \mathcal{D}iag\{\ldots, Z_1, \ldots, Z_2\}$ and $A_S = \mathcal{D}iag\{\ldots, Z_3, \ldots, Z_4\}$, where $Z_1 = I_{A_B\times A_B}$, $Z_2 = 0_{A_S\times A_S}$, $Z_3 = 0_{A_B\times A_B}$ and $Z_4 = I_{A_S\times A_S}$.

After this, we could get the convex relaxation of extend optimization problem $(EOP1)$ as

$$\begin{aligned}(EOP2)\quad &\max_{\{\omega_j\}_{j=1}^{J_G},\{\nu_j\}_{j=1}^{J_G},\gamma_{0,J}} \sum_{j=1}^{J_G}\log(1+\gamma_{0,J})\\ &s.t.\ C1\!:\quad P_{B,I} = \sum_{j=1}^{J_G} tr(A_{B,I}\Omega_{joint,J}^H\\ &\qquad\qquad \Omega_{joint,J}) \leq P_{B,i,I,max} I \in [1, I_B]\\ &\quad C2\!:\quad P_S = \sum_{j=1}^{J_G} tr(A_S\Omega_{joint,J}^H\Omega_{joint,J})\\ &\qquad\qquad \leq P_{S,max}\\ &\quad C3\!:\quad \sum_{J=1}^{J_G}\{\underline{R}_{B,I,J,K}s_J + \underline{s}_J R_{B,I,J,K}\\ &\qquad\qquad - \underline{s}_J\underline{R}_{B,I,J,K}, \bar{R}_{B,I,J,K}s_J\\ &\qquad\qquad + \bar{s}_J R_{B,I,J,K} - \bar{s}_J\bar{R}_{B,I,J,K}\} \leq C_I\\ &\quad C4: \Omega_{joint,J} \in\\ &\qquad\qquad \mathcal{C}onv\left(\mathcal{W}_{I,J,K}^{[\underline{\theta}_{I,J,K},\bar{\theta}_{I,J,K}]}(\gamma_{0,J})\right)\end{aligned}$$

Up to here, we get the relaxation of the extend optimization problem $(EOP2)$ which is a second-order cone programming (SOCP) problem, it could be solved by using interior-point method according to [31]. But in the relaxation steps towards $(EOP2)$, we use the method of convex envelope and assume the range of the variables. So we need to solve the upper bound and lower bound in order to satisfy the constraints.

We denote $d = [s, R, \theta] \in \mathbb{R}_+^{N_d}$ as the variable vector that includes our interest factors in it where $N_d = (I_B + 1)J_G + I_B J_G + I_B J_G$. Here the factor R represents $R(\gamma_{0,J})$, specifically, $R_{I,J,K}$ represents the correct user K in group J of base station I, because the logarithm function of $\log(1+\gamma_{0,J})$ keeps the monotonicity of $\gamma_{0,J}$, so we could use the R instead of $\gamma_{0,J}$. Researchers in [31] gave the proof that d belongs to the rectangle $D = [\underline{d}, \bar{d}]$. So we let R^t represent the list of rectangle D, let Θ_U^t and Θ_L^t represent the upper bound and lower bound of the extend optimization problem at the $t-$th iteration. Let $\Theta_U(D)$ and $\Theta_L(D)$ denote the upper bound and lower bound of the the certain rectangle range D.

So, when the iteration meats the $t-$th times, we need to select a rectangle in R^t and split it into two small rectangles. But the selection from R^t have many options that a good method could decrease the time and computation. Here we choose the rectangle with the largest upper bound [32]. We assume the rectangle is $D^* = [l, u]$, after that, we divide it into two small parts along the longest edge with equal size as

$$\begin{aligned}D_{(1)}^* &= \begin{cases}[l, u - e_{j*}], & j^* \leq (I_B+1)J_G,\\ [l, u - (u_{j*} - l_{j*})/2 \times e_{j*}], & otherwise,\end{cases}\\ D_{(2)}^* &= \begin{cases}[l + e_{j*}, u], & j^* \leq (I_B+1)J_G,\\ [l + (u_{j*} - l_{j*})/2 \times e_{j*}, u], & otherwise,\end{cases}\end{aligned} \tag{19}$$

where e_{j*} is the j^*-th standard basis vector. This method could add the new rectangle $D \in \{D_{(1)}^*, D_{(2)}^*\}$ into consideration, and update the upper bound Θ_U^{t+1} and lower bound Θ_L^{t+1} in time. So after one iteration, new rectangle $D \in \{D_{(1)}^*, D_{(2)}^*\}$ could be used to update the upper bound and lower bound.

As illustrated in the last paragraph, the effective method to select suitable rectangle D is to choose the one with the largest upper bound, such as $D^* = argmax_{D\in R^t}\Theta_U(D)$, and if we select the rectangle along the longest edge such as $j^* = argmax_{j\in[1,N_d]}\{u_j - l_j\}$, then we could compute the upper bound $\Theta_U(D)$ by solving the problem $(EOP2)$ over the rectangle D referring to [34]. For updating the upper bound during the iteration, for each time that we obtain new $D \in \{D_{(1)}^*, D_{(2)}^*\}$, we could form R^{t+1} by removing old D^* from D^t and then add new $D_{(1)}^*$ and $D_{(2)}^*$ if the new upper bound is larger than the lower bound. We could formulate this step as

$$R^{t+1} = R^t \backslash D^* \cup \{D_{(1)}^*, D_{(2)}^* | \Theta_U(D_{(1)}^*, D_{(2)}^*) \geq \Theta_L\} \tag{20}$$

So we could update the upper bound as

$$\Theta_U^{t+1} = \max_{D\in R^{t+1}} \Theta_U(D) \tag{21}$$

Next is the lower bound. For obtaining a lower bound, we should first find a feasible solution of $(EOP2)$. Because of the backhaul links exist, we could control the transmit power of some groups and keep the other groups active. We know that, if $||\omega_{I,J}||^2 \neq 0$ the backhaul link factor $s_J = 1$, otherwise $s_J = 0$. So in extreme cases, the small enough but not zero beamforming vector $||\omega^*_{I,J}||^2$ exist, $s_J = 1$ but contribute little to the capacity. Therefore, we denote power factor p_J as the $j-$th largest factor of $\Omega_{joint,J}$, and define

$$\tilde{\Omega}_{joint,J} = \begin{cases} 0, & ||\omega^*_{I,J}||^2 < p_J, \\ \omega^*_{I,J}, & otherwise, \end{cases}$$
$$\tilde{s}_J = \begin{cases} 0, & ||\omega^*_{I,J}||^2 < p_J, \\ 1, & otherwise, \end{cases} \quad (22)$$

Then we could obtain the capacity as

$$R_{I,J,K}(\tilde{\Omega}_{joint,J}) = \log_2(1+\frac{|h_{joint,J}\tilde{\Omega}_{joint,J}|^2}{\sum_{\substack{j=1\\j\neq J}}^{J_G}|h_{joint,J}\tilde{\Omega}_{joint,J}|^2+\sigma^2}) \quad (23)$$

And if the backhaul constraint is satisfied, then it could be written as

$$\sum_{J=1}^{J_G}\tilde{s}_J R_{B,I,J,K}(\tilde{\Omega}_{joint,J}) \leq C_I, \quad I \in [0, I_B] \quad (24)$$

then $\{\tilde{s}_J, \tilde{\Omega}_{joint,J}, R_{I,J,K}(\tilde{\Omega}_{joint,J})\}$ is a feasible solution of the extend optimization problem $(EOP2)$. Otherwise, we can scale $\{R_{I,J,K}(\tilde{\Omega}_{joint,J})\}$ to be the feasible solution of $(EOP2)$ as

$$\tilde{R}_{I,J,K} = \min\left\{\min\frac{C_I}{\sum\limits_{J=1}^{J_G}\tilde{s}_J R_{B,I,J,K}(\tilde{\Omega}_{joint,J})}, 1\right\} \times R_{I,J,K}(\tilde{\Omega}_{joint,J}) \quad (25)$$

This means there definitely exists a factor that help us obtain the lower bound of the extend optimization problem as

$$\Theta_L(D) = \max_{s_J, J\in[1,(I_B+1)J_G]}\{\Theta_L^J(D)\} \quad (26)$$

In the iteration, if the new step could provide new rectangle that have a larger lower bound than previous steps, then we update the lower bound with

$$\Theta_L^{t+1} = \max\{\Theta_L(D^*_{(1)}), \Theta_L(D^*_{(2)}), \Theta_L^t\} \quad (27)$$

So we summarize the Bound-base Algorithm as **Algorithm 2**.

Algorithm 2 Bound-Based Algorithm

1. **Initialize:** $R^0 \leftarrow \{D_{init}\}$, $t \leftarrow 0$, solving $(EOP2)$ for upper bound $\Theta_U(D_{init})$ and obtain the lower bound $\Theta_L(D_{init})$ according to (21). $\Theta_L^0 = \Theta_L(D_{init})$, $\Theta_U^0 = \Theta_U(D_{init})$, ϵ.
2. **while do** $\Theta_U^t - \Theta_L^t > \epsilon$
3. Select the rectangle D^* in R^t with the largest upper bound, and split it into $D^*_{(1)}$ and $D^*_{(2)}$ according to (19).
4. Calculate upper bound $\Theta_U(D^*_{(1)}, D^*_{(2)})$ by solving $(EOP2)$ and lower bound $\Theta_L(D^*_{(1)}, D^*_{(2)})$ according to (26).
5. **Update** $R^{t+1} = R^t \backslash D^* \cup \{D^*_{(1)}, D^*_{(2)} | \Theta_U(D^*_{(1)}, D^*_{(2)}) \geq \Theta_L\}$.
6. **Update** $\Theta_U^{t+1} = \max_{D\in R^{t+1}}\Theta_U(D)$.
7. **Update** $\Theta_L^{t+1} = \max\{\Theta_L(D^*_{(1)}), \Theta_L(D^*_{(2)}), \Theta_L^t\}$
8. t = t + 1.
9. **End While**

B. Low-Complexity Heuristic Transformation

In previous subsection, we propose the Bound-based algorithm to obtain the upper bound of the problem. But from the analysis we know that, the complexity of this algorithm is high, so we propose a low-complexity heuristic algorithm in this subsection to solve the problem.

In the Bound-based algorithm, the most complex steps are the convex envelope shrinking especially the constraints $C3$ and $C4$ in $(EOP2)$. So we could focus on these two constraints to heuristic the algorithm. We first rewrite the constraint $C4$ in $(EOP1)$ as

$$\underbrace{\sum_{\substack{j=1\\j\neq J}}^{J_G}|h_{joint,I,J,K}\Omega_{joint,J}|^2+\sigma_N^2}_{\text{convex}} - \underbrace{\frac{|h_{joint,I,J,K}\Omega_{joint,J}|^2}{\Gamma_{I,J,K}\gamma_{0,J}}}_{\text{convex}} \leq 0 \quad (28)$$

From [33] we know that, the two parts of equation (28) are convex. But the total difference equation is uncertain convex or non-convex. Referring to the optimization of equation (11), we could replace it into the first-order Taylor expansions form as

$$\sum_{\substack{j=1\\j\neq J}}^{J_G}|h_{joint,I,J,K}\Omega_{joint,J}|^2 + \sigma_N^2 - \frac{2\mathcal{R}e\{\Omega^{(*)H}_{joint,J}h^H_{joint,I,J,K}h_{joint,I,J,K}\Omega_{joint,J}\}}{\Gamma_{I,J,K}\gamma^{(*)}_{0,J}} + \frac{|h_{joint,I,J,K}\Omega^{(*)}_{joint,J}|^2}{(\Gamma_{I,J,K}\gamma^{(*)}_{0,J})^2} \leq 0 \quad (29)$$

For constraint $(C3)$ in $(EOP1)$, to keep the form consistent, we could rewrite it as

$$\sum_{J=1}^{J_G}[(s'_J+R'_{B,I,J,K})^2-(s'_J-R'_{B,I,J,K})^2] \leq 4C_I I \in [0, I_B] \quad (30)$$

where $s'_J \geq u_J tr(A_J\Omega^H_{joint,J}\Omega_{joint,J})$ and $R'_{B,I,J,K} \geq R_{B,I,J,K}$. We notice that for any a and b there has $4ab = (a+b)^2 - (a-b)^2$. So we finally have the heuristic form

Algorithm 3 Heuristic Algorithm

1: **Initialize:** $\Omega^{(0)}_{joint,J}$, $\gamma^{(0)}_{0,J}$, $s'^{(0)}_J$, $R'^{(0)}_{B,I,J,K}$ and $t=0$, set the iteration threshold ϵ.
2: **repeat**
3: Solve the heuristic problem $(HP)^{(t)}$ and update $\Omega^{(t)}_{joint,J}$, $\gamma^{(t)}_{0,J}$, $s'^{(t)}_J$, $R'^{(t)}_{B,I,J,K}$.
4: t=t+1
5: **until** the stopping criterion is met.

below:

$$
\begin{aligned}
(HP)\quad & \max_{\{\omega_j\}_{j=1}^{J_G},\{\nu_j\}_{j=1}^{J_G},\gamma_{0,J},\psi,\phi} \sum_{j=1}^{J_G}\log(1+\gamma_{0,J})\\
& s.t.\ C1\colon\ P_{B,I}=\sum_{j=1}^{J_G} tr(A_{B,I}\Omega^H_{joint,j}\Omega_{joint,j})\\
&\qquad \le P_{B,i,I,max} I\in[1,I_B]\\
& C2\colon\ P_S=\sum_{j=1}^{J_G} tr(A_S\Omega^H_{joint,J}\Omega_{joint,J})\le P_{S,max}\\
& C3\colon\ \sum_{J=1}^{J_G}[(s'_J+R'_{B,I,J,K})^2-2(s'^{(t)}_J-R'^{(t)}_{B,I,J,K})\\
&\qquad \times(s'_J-R'_{B,I,J,K})+(s'^{(t)}_J-R'^{(t)}_{B,I,J,K})^2]\le 4C_I\\
& C4\colon\ \sum_{\substack{j=1\\ j\ne J}}^{J_G}|h_{joint,I,J,K}\Omega_{joint,J}|^2+\sigma_N^2\\
&\qquad -\frac{2\mathcal{R}e\{\Omega^{(t)H}_{joint,J}h^H_{joint,I,J,K}h_{joint,I,J,K}\Omega_{joint,J}\}}{\Gamma_{I,J,K}\gamma^{(t)}_{0,J}}\\
&\qquad +\frac{|h_{joint,I,J,K}\Omega^{(t)}_{joint,J}|^2}{(\Gamma_{I,J,K}\gamma^{(t)}_{0,J})^2}\le 0
\end{aligned}
$$

Thus the heuristic problem (HP) is convex referring to [33], our target is to obtain $\Omega^{(t)}_{joint,J}$, $\gamma^{(t)}_{0,J}$, $s'^{(t)}_J$, $R'^{(t)}_{B,I,J,K}$ in which t is the iteration times. We could solve by using interior-point methods [28] that a feasible solution could be optimized by random initialization points. The low-complexity heuristic algorithm is given in **Algorithm 3**.

C. Convergence and Complexity Analysis

1) *Convergence of Bound-based algorithm:* In previous subsections, we use the upper bound and lower bound to gain the optimization solution, so the most important condition is the convergence of the algorithm. If the upper bound and lower bound over the rectangle D could become tight and finally shrink to a point, then the convergency of the algorithm is valid. Research [35] first gave the proof of the convergence that rectangle D shrinks to a point. We refer the method to prove our formulation and bounds in **Appendix**.
2) *Complexity of Algorithm 1,* 2 *and 3:* For these three algorithms, the most complex parts are the iteration cycles in them, so the complexity analysing could be mainly calculated by iteration times and iteration steps complexity. The complexity of three algorithms are $\mathcal{O}(T_1^{max}(((I_BA_B)^2+A_S^2)J_G+K_U)^{3.5})$, $\mathcal{O}(T_2^{max}((I_BA_B+A_S)J_GK_U)^{3.5}$ and $\mathcal{O}(T_3^{max}((I_BA_B+A_S)J_GK_U)^{3.5}$. Referring to [34], $T_2^{max}\gg T_3^{max}, T_2^{max}\gg T_1^{max}$, thus the iteration time could better represent the complexity of the algorithms. Further comparisons are stated in the next section.

V. Performance Evaluation

In this section, we use the MATLAB software to simulate and evaluate the proposed algorithm and then present the result. Here we first give the simulation parameters, and then give the simulation results and analysis.

A. Simulation Parameters

In the simulation, the satellite is a LEO with $1000km$ from the ground, the maximum power is 40W, and the carrier frequency is set as 2GHz, the AWGN power σ_N is set as $-134dBm$. The maximum constraint power of the base stations $P_{B,i,I,max}$ is set as $43dBm$. The transmission gain of the satellite and the base station are $50dBi$ and $18dBi$. The ground users' position is assumed as Gaussian distribution.

Meanwhile, for the transmission channel, the channel fading should be considered. In this model, we assume the terrestrial channel as Rayleigh channel [36], and the satellite channel as Rician channel [37]. To keep the scenario more realistic, we also consider shadow effect that caused by the environment. Refereing to [38] and [39], the Probability Density Function (PDF) of terrestrial and satellite channel model could be written as

$$
\begin{aligned}
p_B(x) &= \frac{10}{ln(10)\sqrt{2\pi\sigma^2}}\int_0^\infty \frac{1}{x_0^2}\\
&\quad\times \exp[-\frac{x}{x_0}-\frac{(10\log(x_0)-\mu)^2}{2x_0}]dx_0\\
p_S(x) &= \frac{x}{\sigma\sqrt{2\pi\sigma^2}}\int_0^\infty \frac{1}{x}\\
&\quad\times \exp[-\frac{\ln x_0-\mu}{2\sigma^2}-\frac{(x^2+x_0^2)}{2\sigma}]I_0(\frac{xx_0}{\sigma})dx_0
\end{aligned}
$$

where x_0 is the mean power of signal that under short time shadow effect, μ and σ are mean and variance of signal, I_0 is the first kind zero-order modified Bessel function.

B. Simulation Results and Analysis

Fig.2 shows the convergence of **Algorithm 1**, **Algorithm 2** and **Algorithm 3**. In Fig.2 (a), when the base station number, group size and group number increase, the time of iteration increases too. This is because the complexity of group forms influences the cooperative optimization, it need more chances to reach the final result. From the figure we could see, **Algorithm 1** needs 14 to 15 iteration times to gain the convergence. Fig.2(b) shows the convergence of **Algorithm 2**. The condition is $I_B=2, J_G=1, K_U=2, \Gamma_{I,J,K}=1$. From this figure, we could see that the upper bound is decreases very fast during the start iteration times, and gradually decreases

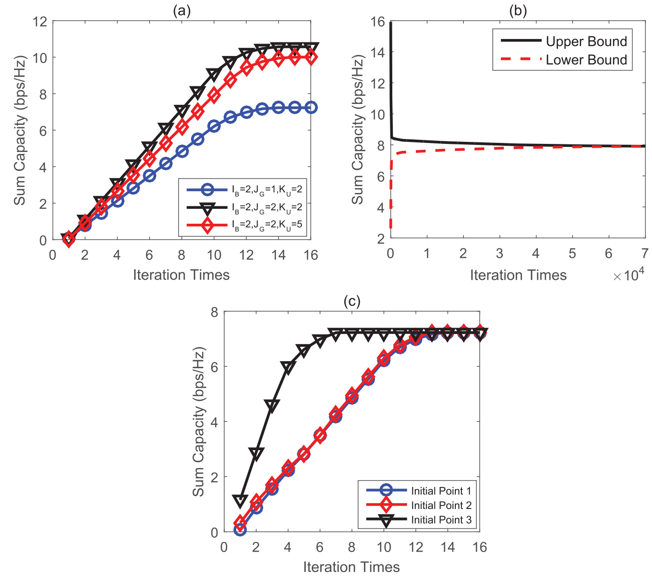

Fig. 2. Convergence Behavior of Algorithm 1, Algorithm 2 and Algorithm 3.

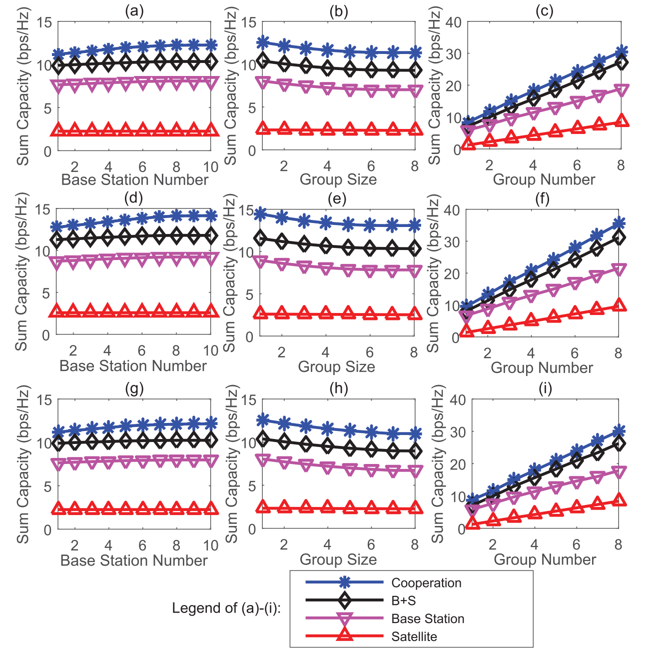

Fig. 3. Performance of Algorithm 1, Algorithm 2 and Algorithm 3.

slower and slower, at the end comes to a correct value. Same as the lower bound that it increases very fast at the beginning and slow down after that until reach a correct value. We also see that, when the iteration comes to the end, the upper bound and lower bound become tight according to the stopping tolerance factor ϵ. The ϵ smaller, the gap between two bounds nearer. Fig.2 (c) shows the convergence of **Algorithm 3** with $I_B = 2, J_G = 1, K_U = 2, \Gamma_{I,J,K} = 1$. From this figure we find that, different initial points lead to different iteration times but the algorithm finally become convergence in 14 times. From these three figures we also could find that the complexity of **Algorithm 3** is the lowest, then is **Algorithm 1**, and **Algorithm 2** has the highest complexity which has been illustrated in previous section, and the achieved results in (b) could still be used as the benchmark of the total system capacity.

Fig.3 shows the performance of our proposed **Algorithm 1**, **Algorithm 2** and **Algorithm 3** under the influence of base station number, group size and group number. To see the differences more clearly, we put all the nine subfigures together. The top subfigures (a) (b) and (c) represent the total system capacity of **Algorithm 1**, and the bottom subfigures (d) (e) and (f) represent the performance of **Algorithm 2**, (g) (h) (i) are for **Algorithm 3**. In (a), (d) and (g) we set $A_B = 2, A_S = 4, K_U = 2, J_G = 2, \Gamma_{I,J,K} = 1$, in (b), (e) and (h) we set $A_B = 2, A_S = 4, I_B = 2, J_G = 2, \Gamma_{I,J,K} = 1$, and in (c), (f) and (i) we set $A_B = 2, A_S = 4, I_B = 2, K_U = 2, \Gamma_{I,J,K} = 1$. From the first column we find that, more base station number provide better channel for the ground users, so the sum capacity increase. From the second column we know, the group size increases, the sum capacity may decrease. Because if there are more users, the minimum SINR of each group might be worse and the interference might be higher according to the increment of group size. From the third column, all the four lines present increment. This is because the group number increases, the sum capacity increases obviously. But further observing these subfigures,

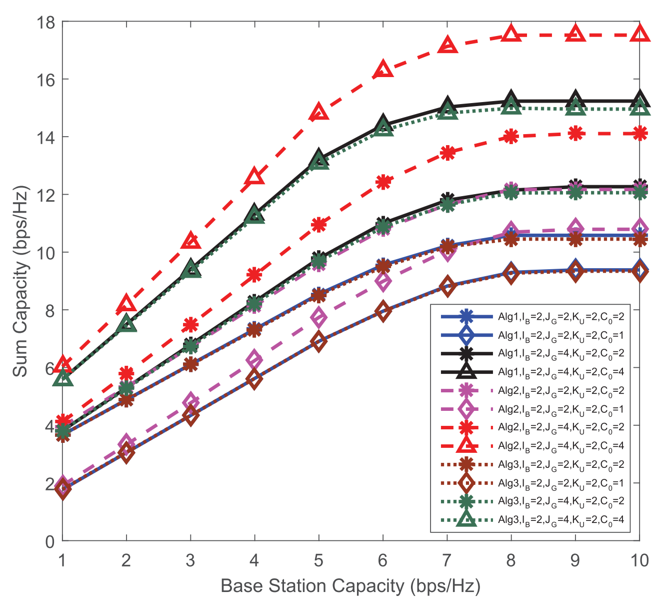

Fig. 4. Sum capacity under different backhaul capacity constraints.

the slope of them are very small. The reason is that, when the group number increases, the interference between groups rise very fast. Meanwhile, observing all the nine subfigures, we could see that, the blue asterisk line is higher than the black diamond line. It means the ability of cooperative optimization is better than non-cooperative optimization. And the gain of **Algorithm 1** is about 18.5% in (a), 22.4% in (b) and 11.9% in (c). Compared with **Algorithm 1**, the bound-based **Algorithm 2** obtains nearly 15% capacity, and **Algorithm 3** is 1.6% less than **Algorithm 1**.

Fig.4 shows the influence of the backhaul capacity constraint. In this figure, the x-axis represents the base station backhaul capacity, and we compare the two algorithms with different satellite backhaul capacity at the same time. It is

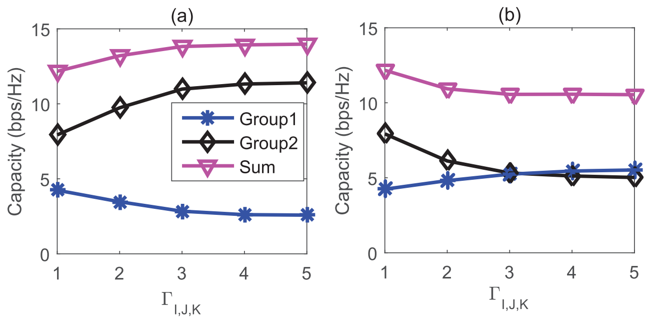

Fig. 5. Influence of $\Gamma_{I,J,K}$.

obviously that all the lines increase nearly linear at the beginning, slow down and keep flat when the backhaul capacity rises. Because when the backhaul capacity is small, only few groups are under service or the groups are under bad quality of service, so as the capacity grows, the total system capacity increase fast. And when the backhaul capacity is large enough, all the groups have already been under service or the groups have already under good quality of service, at this time the influence of backhaul capacity is less. Since all the groups are under the best optimization, the total system capacity would not rise. And comparing the lines in same line style, we could find the influence of different satellite backhaul capacity. Comparing the lines in same line marks in same algorithm, we could find the different tendency of increment with different group number. And comparing the lines in same line marks in different algorithms, we could find the tendency of increment with different algorithm.

Fig.5 shows the influence of the target SINR factor $\Gamma_{I,J,K}$. We set the factors as $A_B = 2, A_S = 4, I_B = 2, J_G = 2, K_U = 2$. In subfigure (a), we set the target SINR of group 1 as $\Gamma_{I,J,K} = 1$ and the target SINR of group 2 as $\Gamma_{I,J,K} = \Gamma_x$ in which Γ_x represents the x-axis of this subfigure. In subfigure (b), we set the target SINR of group 2 as $\Gamma_{I,J,K} = 1$ and the target SINR of group 1 as $\Gamma_{I,J,K} = \Gamma_x$ in which Γ_x represents the x-axis of this subfigure. From the two subfigures we find that, when the two groups are all $\Gamma_{I,J,K} = 1$, the capacity of group 2 is larger than group 1. It means that, under the same service grade, the channel condition of group 2 is better. When the $\Gamma_{I,J,K}$ increases in (a), the resource is allocated more to the group 2 obviously, and the increment of group 2 is larger than the decline of group 1. In (b), the condition is opposite that the speed of decline of group 2 is faster than increment of group 1. The influence to the group under better channel condition of $\Gamma_{I,J,K}$ is larger than it of bad channel condition group. So we could adjust this factor to obtain the different requirements under different application scenarios.

Fig.6 is the comparison of our proposed **Algorithm 1**, **Algorithm 2**, **Algorithm 3**, suboptimization method in [16] and maximum-ratio-transmission (MRT) method. Comparing these methods, we find that, the **Algorithm 1** gains 14.9% more capacity than the suboptimization method, and gains 35.1% more capacity than the MRT. The **Algorithm 2** obtains the correct bound and optimizes the problem as the benchmark of capacity. **Algorithm 3** is very close to **Algorithm 1** when x-axis is small, along with x-axis gets higher, **Algorithm 3** is

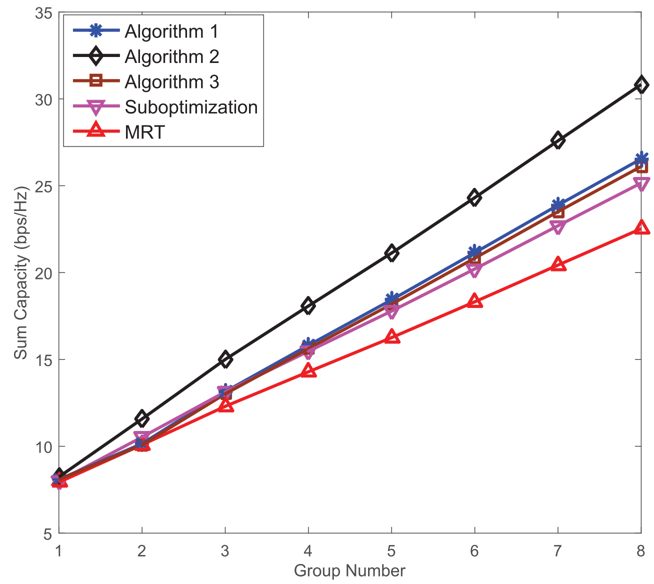

Fig. 6. Comparison of Different Algorithms.

1.6% less than **Algorithm 1**. Meanwhile, compared with **Algorithm 2**, **Algorithm 1** is 13% less, **Algorithm 3** is 15.3% less, suboptimization method and MRT are 18.4% and 26.9% less. **Algorithm 2** could be treated as benchmark is because during convex transformation, the constraints reform are all based on the physical property. We use the arguments of beams to set the convex envelope such as equation (15), the transformation based on arguments has very little component loss. But in **Algorithm 1** and **Algorithm 3**, we expansion the constraints by first-order, there are many components that are dropped by this relaxation step. Besides, the MRT method could not deal with the complex interference, so when the interference of groups get higher, the performance of it would be the worst. The method in [16] solve the problem using suboptimization function, this might get stuck in unfavorable local solutions. And for the cooperative optimization, the ability of this method is not good enough.

Another important factor we are interest in is the influence of system delay of terrestrial channel and satellite channel. It seems that the satellite and base stations could not be managed at the same time, at least could not keep a high synchronization. In fact, according to [40], the low time delay satellite transmission technology had been studied. Meanwhile, the development of ground mobile terminals aims at high intelligent and computing complex, they could communicate with satellite only by one or two hops, this means the transmission delay of satellite could be shortened in dozens of millisecond. Taking the terrestrial link into consideration, most base stations are only relay stations. The ground users could not communicate with control center or content center directly, on the contrary, it needs dozens of hops [41]. Under this condition, the satellite delay is not high and even low than the terrestrial delay. To schedule the network more accurately, we could further research the allocation schemes to keep up with the delay of satellite and terrestrial network, but it is beyond the scope of this paper, we would study this in future work.

VI. Conclusion

In this paper, we proposed a multicast beamforming terrestrial-satellite cooperation system to maximize the sum of user minimum ratio under the SINR constraint and back-haul link capacity constraint. In this model, satellite and base stations provided service corporately for ground users. We first formulated the optimization problem and then solved it with the proposed joint iterative beamforming design and resource allocation algorithm which was based on SCA and iteration method. After that, we proposed a bound-based algorithm to obtain the upper bound and lower bound of the optimization problem and gained the result that could be treated as the benchmark of the same problem. Then to decrease the complexity of bound-based method, we designed a heuristic algorithm to resolve the problem. During the solution, we further considered the physical property of beams to obtain higher performance. Finally we simulated the two proposed algorithms and compared them with previous literatures. The simulation results showed that, our proposed cooperative optimization algorithms had better performance than non-cooperative methods, and the heuristic scheme had little poor performance but had significant advantage in low complexity. In this paper, we only considered the optimization method without time-varying which including the movement of users and satellite, in the future, we would further study the influence of time-varying and take transmission delay into account to design the system more realistic.

Appendix

From equation (13) and (15), we have

$$\frac{|h_{joint,I,J,K}\Omega_{joint,J}|^2}{\sum_{\substack{j=1\\ j\neq J}}^{J_G}|h_{joint,I,J,K}\Omega_{joint,J}|^2+\sigma_N^2} \geq (\underline{\gamma}_{0,J})\cos^2\left(\frac{\bar{\theta}_{I,J,K}-\underline{\theta}_{I,J,K}}{2}\right)$$

Refer to [25], for any $D \in D_{init}$, we assume $D = [l, u]$ that $l = [\underline{s}_J^H, \underline{R}_J^H, \underline{\theta}_{I,J,K}^H]^H$ and $u = [\bar{s}_J^H, \bar{R}_J^H, \bar{\theta}_{I,J,K}^H]^H$. If we denote the longest edge of the rectangle D as $EDGE(D)$, then $EDGE(D) \leq \delta$ means $\max_{1\leq J\leq N_d}\{u_J - l_J\} \leq \delta$. Based on this result, the initial bound $\Theta_L(D)$ and $\Theta_U(D)$ could be estimated first.

Upper Bound: We define $\{\Omega_{joint,J}^*, R_J^*, s_J^*\}$ as the optimal solution of $(EOP2)$ that after solving this problem we have the upper bound $\Theta_U(D) = \sum_J R_J^*$, and the upper bound satisfies $\Theta_U(D) \leq \sum_J \bar{R}_J$.

Lower Bound: Since the size of rectangle D is small enough that $\delta \leq 1$, we have $\underline{s}_J = \bar{s}_J$ by (19). If this satisfies, the optimal solution is $s_J^* = \underline{s}_J = \bar{s}_J = 0$ *or* 1. According to (22), we assume there exists the smallest non-zero element of $||\Omega_{joint,J}||^2$, then $\bar{s}_J = s_J^*$ and $\bar{\Omega}_{joint,J} = \Omega_{joint,J}^*$. So we have

$$\frac{|h_{joint,I,J,K}\Omega_{joint,J}^*|^2}{\sum_{\substack{j=1\\ j\neq J}}^{J_G}|h_{joint,I,J,K}\Omega_{joint,J}^*|^2+\sigma_N^2} \geq (\underline{\gamma}_{0,J})\cos^2\left(\frac{\bar{\theta}_{I,J,K}-\underline{\theta}_{I,J,K}}{2}\right)$$

Then the capacity satisfies

$$\begin{aligned}
&R_{I,J,K}(\bar{\Omega}_{joint,J})\\
&\quad= R_{I,J,K}(\Omega_{joint,J}^*)\\
&\quad= \min\log_2\left(1+\frac{|h_{joint,I,J,K}\bar{\Omega}_{joint,J}|^2}{\sum_{\substack{j=1\\ j\neq J}}^{J_G}|h_{joint,I,J,K}\bar{\Omega}_{joint,J}|^2+\sigma_N^2}\right)\\
&\quad\geq \min\log_2\left(1+\underline{\gamma}_{0,J}\cos^2\left(\frac{\bar{\theta}_{I,J,K}-\underline{\theta}_{I,J,K}}{2}\right)\right)\\
&\quad= \log_2\left(1+\underline{\gamma}_{0,J}\cos^2\left(\frac{\max(\bar{\theta}_{I,J,K}-\underline{\theta}_{I,J,K})}{2}\right)\right)\\
&\quad= \log_2\left(1+(2^{\underline{R}_{I,J,K}}-1)\cos^2\left(\frac{\max(\bar{\theta}_{I,J,K}-\underline{\theta}_{I,J,K})}{2}\right)\right)\\
&\quad\geq \log_2\left(\underline{R}_{I,J,K}\cos^2\left(\frac{\max(\bar{\theta}_{I,J,K}-\underline{\theta}_{I,J,K})}{2}\right)\right)\\
&\quad= \underline{R}_{I,J,K}+2\left(\cos\left(\frac{\max(\bar{\theta}_{I,J,K}-\underline{\theta}_{I,J,K})}{2}\right)\right)
\end{aligned}$$

And the lower bound is given by $\Theta_L(D) = \sum_J \underline{R}_J$.

Finally, the gap between upper bound and lower bound is

$$\begin{aligned}
&\Theta_U(D)-\Theta_L(D)\\
&\quad= \sum_J(R_J^*-\underline{R}_J)\\
&\quad\leq \sum_J(\bar{R}_J-\underline{R}_J)-\left(\cos\left(\frac{\max(\bar{\theta}_{I,J,K}-\underline{\theta}_{I,J,K})}{2}\right)\right)\\
&\quad\leq I_B J_G\delta-\log_2\big(\cos(\delta/2)\big)
\end{aligned}$$

where we denote $g(\theta) = I_B J_G\delta - \log_2\big(\cos(\delta/2)\big)$ is monotonically increasing for $\delta \in (0, 1)$, there always exists a small enough δ that satisfies $g(\theta) \leq \epsilon$.

The proof is completed.

References

[1] W. Obile, "Ericsson mobility report," Ericsson, Stockholm, Sweden, Tech. Rep. EAB-16:001237, Nov. 2016.

[2] Cisco, "Cisco visual networking index: Global mobile data traffic forecast update 2014–2019," Cisco VNI, San Jose, CA, USA, White Paper C11-520862, Feb. 2015.

[3] T. L. Marzetta, "Noncooperative cellular wireless with unlimited numbers of base station antennas," *IEEE Trans. Wireless Commun.*, vol. 9, no. 11, pp. 3590–3600, Nov. 2010.

[4] F. Rusek *et al.*, "Scaling up MIMO: Opportunities and challenges with very large arrays," *IEEE Signal Process. Mag.*, vol. 30, no. 1, pp. 40–60, Jan. 2013.

[5] J. Hoydis, S. ten Brink, and M. Debbah, "Massive MIMO in the UL/DL of cellular networks: How many antennas do we need," *IEEE J. Sel. Areas Commun.*, vol. 31, no. 2, pp. 160–171, Feb. 2013.

[6] S. Yang and L. Hanzo, "Fifty years of MIMO detection: The road to large-scale MIMOs," *IEEE Commun. Surveys Tuts.*, vol. 17, no. 4, pp. 1941–1988, 4th Quart., 2015.

[7] F. Z. Merli, X. Wang, and G. M. Vitetta, "Low-rate-feedback-assisted beamforming and power control for MIMO-OFDM systems," *IEEE Trans. Veh. Technol.*, vol. 59, no. 1, pp. 225–234, Jan. 2010.

[8] S. Han, Y. Zhang, W. Meng, and H.-H. Chen, "Self-interference-cancelation-based SLNR precoding design for full-duplex relay-assisted system," *IEEE Trans. Veh. Technol.*, vol. 67, no. 9, pp. 8249–8262, Sep. 2018.

[9] *3rd Generation Partnership Project; Tech. Specification Group Radio Access Network; Study Elevation Beamforming/Full-Dimension (FD) Multiple Input Multiple Output (MIMO) for LTE (Release 13)*, document TR 36.897 v13.0.0, 3GPP, Jun. 2015.

[10] D. Zhu, B. Li, and P. Liang, "A novel hybrid beamforming algorithm with unified analog beamforming by subspace construction based on partial CSI for massive MIMO-OFDM systems," *IEEE Trans. Commun.*, vol. 65, no. 2, pp. 594–607, Feb. 2017.

[11] K. Zheng, L. Zhao, J. Mei, B. Shao, W. Xiang, and L. Hanzo, "Survey of large-scale MIMO systems," *IEEE Commun. Surveys Tuts.*, vol. 17, no. 3, pp. 1738–1760, 3rd Quart., 2015.

[12] S. Han, S. Xu, W. Meng, and C. Li, "Dense-device-enabled cooperative networks for efficient and secure transmission," *IEEE Netw.*, vol. 32, no. 2, pp. 100–106, Mar./Apr. 2018.

[13] S. Han, Y. Huang, W. Meng, C. Li, N. Xu, and D. Chen, "Optimal power allocation for SCMA downlink systems based on maximum capacity," *IEEE Trans. Commun*, vol. 67, no. 2, pp. 1480–1489, Feb. 2019.

[14] S. Han, S. Xu, W. Meng, and C. Li, "An agile confidential transmission strategy combining big data driven cluster and OBF," *IEEE Trans. Veh. Technol.*, vol. 66, no. 11, pp. 10259–10270, Nov. 2017.

[15] L. Liu and H. Jafarkhani, "Successive transmit beamforming algorithms for multiple-antenna OFDM systems," *IEEE Trans. Wireless Commun.*, vol. 6, no. 4, pp. 1512–1522, Apr. 2007.

[16] Z. Wang, D. W. K. Ng, V. W. S. Wong, and R. Schober, "Robust beamforming design in C-RAN with sigmoidal utility and capacity-limited backhaul," *IEEE Trans. Wireless Commun.*, vol. 16, no. 9, pp. 5583–5598, Sep. 2017.

[17] E. Karipidis, N. Sidiropoulos, and Z.-Q. Luo, "Quality of service and max-min fair transmit beamforming to multiple cochannel multicast groups," *IEEE Trans. Signal Process.*, vol. 56, no. 3, pp. 1268–1279, Mar. 2008.

[18] Z. Xiang, M. Tao, and X. Wang, "Coordinated multicast beamforming in multicell networks," *IEEE Trans. Wireless Commun.*, vol. 12, no. 1, pp. 12–21, Jan. 2013.

[19] B. Hu, C. Hua, C. Chen, X. Ma, and X. Guan, "MUBFP: Multiuser beamforming and partitioning for sum capacity maximization in MIMO systems," *IEEE Trans. Veh. Technol.*, vol. 66, no. 1, pp. 233–245, Jan. 2017.

[20] Y.-F. Liu, C. Lu, M. Tao, and J. Wu, "Joint multicast and unicast beamforming for the MISO downlink interference channel," in *Proc. IEEE 18th Int. Workshop Signal Process. Adv. Wireless Commun. (SPAWC)*, Sapporo, Japan, Jul. 2017, pp. 1–5.

[21] J. Du, C. Jiang, Q. Guo, M. Guizani, and Y. Ren, "Cooperative earth observation through complex space information networks," *IEEE Trans. Wireless Commun.*, vol. 23, no. 2, pp. 136–144, Apr. 2016.

[22] J. Du, C. Jiang, J. Wang, Y. Ren, S. Yu, and Z. Han, "Resource allocation in space multiaccess systems," *IEEE Trans. Aerosp. Electron. Syst.*, vol. 53, no. 2, pp. 598–618, Apr. 2017.

[23] X. Zhu, C. Jiang, L. Kuang, N. Ge, and J. Lu, "Non-orthogonal multiple access based integrated terrestrial-satellite networks," *IEEE J. Sel. Areas Commun.*, vol. 35, no. 10, pp. 2253–2267, Oct. 2017.

[24] X. Zhu, C. Jiang, L. Yin, L. Kuang, N. Ge, and J. Lu, "Cooperative multigroup multicast transmission in integrated terrestrial-satellite networks," *IEEE J. Sel. Areas Commun.*, vol. 36, no. 5, pp. 981–992, May 2018.

[25] N. D. Sidiropoulos, T. N. Davidson, and Z.-Q. Luo, "Transmit beamforming for physical-layer multicasting," *IEEE Trans. Signal Process.*, vol. 54, no. 6, pp. 2239–2251, Jun. 2006.

[26] R. Sun, Y. Wang, N. Cheng, H. Zhou, and X. Shen, "QoE driven BS clustering and multicast beamforming in cache-enabled C-RANs," in *Proc. IEEE Int. Conf. Commun. (ICC)*, Kansas City, MO, USA, May 2018, pp. 1–6.

[27] Y. Chen, S. He, Y. Huang, J. Ren, and L. Yang, "Robust multigroup multicast beamforming design for backhaul-limited cloud radio access network," *IEEE Signal Process. Lett.*, vol. 26, no. 1, pp. 189–193, Jan. 2019.

[28] S. Boyd and L. Vandenberghe, *Convex Optimization*. Cambridge, U.K.: Cambridge Univ. Press, 2004.

[29] M. Grant and S. Boyd, (Mar. 2014). *CVX: MATLAB Software for Disciplined Convex Programming*. [Online]. Available: http://cvxr.com/cvx/

[30] F. A. Al-Khayyal and J. E. Falk, "Jointly constrained biconvex programming," *Math. Oper. Res.*, vol. 8, no. 2, p. 273–286, May 1983.

[31] S. Boyd and J. Mattingley, "Branch and bound methods," in *Constrained Global Optimization: Algorithms and Applications*. Berlin, Germany: Springer, 1987.

[32] E. Chen, M. Tao, and Y.-F. Liu, "Joint base station clustering and beamforming for non-orthogonal multicast and unicast transmission with backhaul constraints," *IEEE Trans. Wireless Commun.*, vol. 17, no. 9, pp. 6265–6279, Sep. 2018.

[33] P. Luong, F. Gagnon, C. Despins, and L.-N. Tran, "Optimal joint remote radio head selection and beamforming design for limited fronthaul C-RAN," *IEEE Trans. Signal Process.*, vol. 65, no. 21, pp. 5605–5620, Nov. 2017.

[34] S. Boyd and J. Mattingley, *Branch and bound methods*, document EE364b course notes, Stanford Univ., Stanford, CA, USA, May 2011.

[35] C. Lu and Y.-F. Liu, "An efficient global algorithm for single-group multicast beamforming," *IEEE Trans. Signal Process.*, vol. 65, no. 14, pp. 3761–3774, Jul. 2017.

[36] M. Sawahashi, Y. Kishiyama, A. Morimoto, D. Nishikawa, and M. Tanno, "Coordinated multipoint transmission/reception techniques for LTE-advanced [coordinated and distributed MIMO]," *IEEE Wireless Commun.*, vol. 17, no. 3, pp. 26–34, Jun. 2010.

[37] V. Garcia, Y. Zhou, and J. Shi, "Coordinated multipoint transmission in dense cellular networks with user-centric adaptive clustering," *IEEE Trans. Wireless Commun.*, vol. 13, no. 8, pp. 4297–4308, Aug. 2014.

[38] C. Loo, "A statistical model for a land mobile satellite link," *IEEE Trans. Veh. Technol.*, vol. VT-34, no. 3, pp. 122–127, Aug. 1985.

[39] E. Lutz, W. Papke, and E. Ploechinger, "Land mobile satellite communications: Channel model, modulation, and error control," in *Proc. ESA Workshop Land Mobile Services Satell.*, 1986, pp. 37–42.

[40] K. Ebina, N. Kataoka, M. Ueba, and H. Mizuno, "Investigation of single-hop connections between user terminals in geostationary mobile satellite communication systems," in *Proc. IEEE Global Telecommun. Conf.*, San Antonio, TX, USA, vol. 4, Nov. 2001, pp. 2764–2768.

[41] S. Atapattu, N. Ross, Y. Jing, Y. He, and J. S. Evans, "Physical-layer security in full-duplex multi-hop multi-user wireless network with relay selection," *IEEE Trans. Wireless Commun.*, vol. 18, no. 2, pp. 1216–1232, Feb. 2019.

Yuandong Zhang (S'18) received the B.S. degree in electronic and engineering from Beihang University, Beijing, China, in 2015. He is currently pursuing the Ph.D. degree with the School of Aerospace Engineering, Tsinghua University, Beijing. His major research interest is integrated terrestrial-satellite networks and wireless multimedia communications.

Liuguo Yin (S'01–M'05) received the M.Eng. and Ph.D. degrees from Tsinghua University, Beijing, China, in 2002 and 2005, respectively. From March 2005 to March 2007, he was a Research Assistant with the School of Aerospace, Tsinghua University. From April 2007 to March 2008, he was an ERCIM Post-Doctoral Fellow with the Norwegian University of Science and Technology (NTNU), Trondheim, Norway. Since 2009, he has been with the School of Information Science and Technology, Tsinghua University, where he is currently a Professor. His research interests include channel coding, joint source-channel coding, aerospace communications, wireless multimedia communication systems, and quantum secure direct communications. He is a member of the IEEE Communications Society.

Chunxiao Jiang (S'09–M'13–SM'15) received the B.S. degree (Hons.) in information engineering from Beihang University in June 2008 and the Ph.D. degree (Hons.) in electronic engineering from Tsinghua University, Beijing, China, in January 2013. From February 2013 to June 2016, he held a post-doctoral position with the Department of Electronic Engineering, Tsinghua University, during which he visited the University of Maryland–College Park and the University of Southampton. He is currently an Associate Professor with the School of Information Science and Technology, Tsinghua University. He was a recipient of the IEEE Globecom Best Paper Award in 2013, the IEEE Global-SIP Best Student Paper Award in 2015, and the IEEE Communications Society Young Author Best Paper Award in 2017.

Yi Qian (M'95–SM'07–F'19) received the Ph.D. degree in electrical engineering from Clemson University, Clemson, SC, USA.

He was a Senior Member of the Scientific Staff and a Technical Advisor with Nortel Networks, Ottawa, ON, Canada, a Senior Systems Engineer and a Technical Advisor with several start-up companies, an Assistant Professor with the University of Puerto Rico at Mayagüez, Mayagüez, Puerto Rico, and a Senior Researcher with the National Institute of Standards and Technology, Gaithersburg, MD, USA. He is currently a Professor with the Department of Electrical and Computer Engineering, University of Nebraska-Lincoln (UNL), Lincoln, NE, USA. He has a successful track record in leading research teams and publishes research results in leading scientific journals and conferences. Several of his recent journal articles on wireless network design and wireless network security are among the most accessed articles in the IEEE Digital Library. His current research interests include information assurance and network security, network design, network modeling, simulation, and performance analysis for next-generation wireless networks, wireless ad hoc and sensor networks, vehicular networks, broadband satellite networks, optical networks, high-speed networks, and the Internet.

Dr. Qian is a member of the ACM. He was a recipient of the Henry Y. Kleinkauf Family Distinguished New Faculty Teaching Award in 2011 and the Holling Family Distinguished Teaching Award from the College of Engineering, UNL, in 2012. He is the Chair of the IEEE Communications Society Technical Committee for Communications and Information Security. He serves on the Editorial Boards of several international journals and magazines, including as the Editor-in-Chief for IEEE WIRELESS COMMUNICATIONS. He was a Distinguished Lecturer for IEEE Vehicular Technology Society. He is currently a Distinguished Lecturer for IEEE Communications Society.